Simulation of Concrete Fracture Using *ABAQUS*

Anastasios M. Ioannides[1], Jun Peng[2] and James R. Swindler Jr.[3]

Abstract

This paper discusses the analytical simulation of crack propagation using the Fictitious Crack Model for notched and unnotched Portland Cement Concrete beam specimens. Parameters such as those controlling the loading conditions, mesh fineness, aspect ratio in the vertical or horizontal directions, and notch to beam thickness ratio are considered. The commercial program *ABAQUS* is used, and simulations are compared to previous analytical and experimental results. A linear elastic investigation is first conducted to test the agreement of the results with the Timoshenko beam theory. Subsequently, an investigation is conducted to test the built-in fracture mechanics capabilities of *ABAQUS* for tracking crack propagation. Since these built-in capabilities are found to be inadequate, the creation of a model from basic elements is pursued. This is accomplished by introducing *JOINTC* elements along the crack plane to model joint interactions. Several series of tabulated results are used to illustrate the advantage of using finite element simulation over conducting laboratory experiments, reflected in the time, effort, and money saved. The application of fracture mechanics to understanding concrete pavement cracking is found to be desirable, practical and feasible. It is argued that the development of a truly mechanistic design procedure hinges on the elimination of long-held empirical concepts, including statistical transfer functions.

Introduction

Pavement analysis and design on the basis of fundamental engineering principles has attracted increased attention in the last decade. Commonly referred to as the mechanistic approach to design, such efforts have been given impetus by the unprecedented progress achieved in recent years in the field of computer engineering. In order to build improved pavements, the pavement community is actively pursuing more mechanistic-based design procedures. Such procedures pertain to mechanics as a branch of physics and are expected to be an improvement over current empirical/ statistical approaches. The objective is to prolong satisfactory long-term performance of pavements, thereby minimizing the considerable investment currently devoted to

[1]Associate Professor, Department of Civil and Environmental Engineering, University of Cincinnati (ML-0071), P.O. Box 210071, Cincinnati, OH 45221-0071; e-mail: Anastasios.Ioannides@UC.Edu

[2]Postdoctoral Research Associate, Department of Civil and Environmental Engineering, University of Cincinnati (ML-0071), P.O. Box 210071, Cincinnati, OH 45221-0071; e-mail: Jun.Peng@UC.Edu

[3] Doctoral Research Associate, Department of Civil and Environmental Engineering, University of Cincinnati (ML-0071), P.O. Box 210071, Cincinnati, OH 45221-0071; e-mail: Swindljr@Email.UC.Edu

these complex structures. Incorporation of the most promising new advances from various engineering disciplines into pavement analysis and design activities holds great potential for aiding this objective.

Major distress problems in Portland Cement Concrete (PCC) pavements generally start with crack propagation caused by the combined effects of traffic loads and environmental stressors, such as moisture and temperature. Even if the nominal stresses of the pavement system are below the elastic limit, local stresses may be above the yield point, because of stress concentrations at cracks or notches. Consequently, crack propagation has an important effect on the structural capacity and durability of PCC pavements. Fracture mechanics, particularly the Fictitious Crack Model (FCM) proposed (Hillerborg *et al.* 1976) to simulate crack propagation, can be an important tool towards a better understanding of crack formation and propagation in pavements, which in turn can provide us with models capable of capturing these phenomena.

This paper focuses on the application of the *ABAQUS/STANDARD* finite element software to tracking crack propagation in simply supported beams. A literature review is presented first, introducing the concept of using fracture mechanics to the study of PCC pavements. Next, a discussion of linear elastic analysis of simply supported beams using *ABAQUS/STANDARD* is presented, followed by a consideration of the built-in capabilities of the software for conducting fracture simulations using the FCM. Analyses presented reveal the shortcomings of the built-in software functions, thereby necessitating the development of an alternative formulation. The latter consists of a series of more elementary components available in the package. This is done in the last section of the paper, and involves the use of the *JOINTC* element.

Literature Review

There appears to be little doubt that PCC specimens fail in fatigue when subjected to either constant or variable amplitude repeated loads. Test results exhibit a considerable scatter, lending credence to the suggestion that fatigue is a stochastic phenomenon. The majority of pavement engineers currently employ Miner's fatigue hypothesis in making fatigue life predictions, but most also acknowledge that this is a matter of expedience rather than acceptance of Miner's validity (Ioannides 1997b). As a result of the unsatisfactory predictive ability of current so-called transfer functions, a failure criterion that can be used to estimate the failure strength of a concrete pavement structure must be developed.

Heterogeneous materials, such as PCC, contain defects, imperfections and other forms of flaws that result from the mixing and placement processes. The existence of such flaws causes stress concentration and redistribution around the discontinuous parts of the material. As a result, the failure strength predicted using conventional strength criteria might not be reliable and may overestimate or underestimate the actual strength of the structure. In order to account for the existence of flaws in the material, fracture mechanics may be pursued, resulting in a more rational approach for assessing the concomitant change in structural capacity (Gettu and Shah 1994).

Following an exhaustive examination of the advantages and limitations of a variety of fracture mechanics options (Ioannides 1997a), the FCM was found to be the most promising for studying the fracture mechanics response and behavior of PCC pavements. This model is based on the assumption that a crack starting to develop in the material is still able to transfer some stress across a small, but finite distance. The zone in which such cohesive forces develop is termed the "process zone;" its size is governed by the applied load, support conditions, and specimen geometry, as well as by certain fracture parameters that are assumed to be intrinsic material properties, like the tensile strength, f_t, and fracture energy, G_f. These fracture parameters, however, have been found to be dependent to varying degrees on specimen size and geometry (Ioannides 1997a). This difficulty may be effectively addressed through the use of similitude concepts (Bache and Vinding 1990), and the principles of dimensional analysis (Ioannides *et al.* 2003).

In a previous investigation at the University of Cincinnati (Ioannides and Sengupta 2003), finite element analysis was used in simulating crack propagation in concrete beams. Experimental data pertaining to the load vs. deflection (P-δ) and the load vs. crack mouth opening (P-CMO) behavior of simply supported PCC beams subjected to a point load at mid-span were reproduced past the elastic limit to failure. Finite element package *GTSTRUDL* was used to generate the flexibility matrix pertaining to the linear elastic aspects of structural response, whereas fracture behavior in accordance with the FCM was examined using *CRACKIT*, a FORTRAN computer program coded during the course of the study. The *GTSTRUDL/CRACKIT* combination was then used to generate numerical analysis data for different beam sizes, and these data were interpreted in dimensionless format. An advantage to this approach is that it obviates the need to perform numerous physical tests that are time consuming and costly.

Unfortunately, extending the aforementioned tools to the case of three-dimensional PCC concrete slabs would be prohibitively cumbersome, which calls for the use of a commercially available package. On the other hand, application of such a package can be verified by comparisons with the existing experimental data, as well as with analytical data obtained using the two-dimensional beam model in *GTSTRUDL/CRACKIT*. The commercial software of choice among pavement engineers appears to be *ABAQUS*, a general-purpose, linear or nonlinear, 1D, 2D, or 3D, static or dynamic finite element code developed by *Hibbitt, Karlsson and Sorensen Inc.* (Hibbitt *et al*. 1994). *ABAQUS* incorporates a comprehensive library of element types and material models. It has been very popular for stress/strain, fatigue, flow and thermal analyses in diverse disciplines, including structural, materials, geotechnical, and hydrosystems engineering. It can be implemented on a variety of computer platforms, but it is ideally suited for execution on a supercomputer. The package consists of the following components: *ABAQUS/STANDARD*; a general purpose finite element program; *ABAQUS/ EXPLICIT*, an explicit dynamics finite element program; and *ABAQUS/POST*, an interactive postprocessor. *ABAQUS/ STANDARD* was found to be more suitable for the purposes of this study, and only results obtained from this component are discussed below.

Linear Elastic Investigation

Investigations in this section retained the simply supported beam considered in the aforementioned *GTSTRUDL/CRACKIT* investigation, whose dimensions were 406x152x38 mm (16x6x1.5 in.). The beam is subjected to a concentrated load applied at its mid-span, and is examined using linear elastic analysis. The beam is subdivided into a series of uniform meshes, as well as several non-uniform meshes.

ABAQUS/STANDARD provides a variety of beam elements that can be used for this purpose, including the *CPS4* element, which is described as a four-noded, bilinear plane stress element, and its reduced integration counterpart *CPS4R* element, which allows for hourglass control. Although hourglassing can plague the solution in some cases, it was found that in this study these two elements give very similar results when tracking the deflection of the beam at mid-span. Moreover, the deflected shapes obtained using the *CPS4* and *CPS4R* with hourglass control are essentially identical. Consequently, only results obtained using the *CPS4* element are discussed here.

At the mid-span of the beam, a concentrated load of 44.5 kN (10 kips) is applied as a static load step of increasing magnitude. This requires at least two parameters: the Initial Time Increment (ITI), and the Time Period of the Step (TPS). Two additional parameters may also be specified: the Minimum Time Increment (MnTI), and the Maximum Time Increment (MxTI), for which there is no default value, i.e., it is left unbounded. The TPS is set at 1.0, for convenience, ensuring that all time values are also prescribed in relative terms. It was found that for these linear elastic analyses, MxTI has no influence on the results, as might have been expected. Changing the maximum displacement or velocity leads to proportional changes in the maximum reactive force as predicted by linear elasticity. The following procedure for selecting these parameters was formulated: it is desired to have about 30 time increments during the entire loading process, each increment lasting 3E-2 relative units of time or 3.33% of the total time; this defines the MxTI. The ITI is set to about 1/5th of this value (6E-3); the MnTI is chosen as approximately 1/5th of the ITI (1E-3).

The mesh fineness for the beam specimens considered may be quantified by the ratio of element size/beam thickness, ($\Delta y/h$). It was observed that upon mesh refinement, deflection increases significantly, and a fineness ratio of approximately 2-3% is recommended. The element aspect ratio, α, is defined as the ratio of the element long side divided by the element short size. Analyses conducted to examine the influence of a progressively coarser mesh away from the mid-span region indicate that as long as the aspect ratio in the x-direction (beam length-wise), α_x, is below about 10, the responses tracked remain unaffected. In contrast, the aspect ratio in the y-direction (beam thickness-wise), α_y, can be as high as 100 or more, without significant deterioration in the results.

A comparison was made between the results obtained using *ABAQUS/ STANDARD* with element *CPS4* and those calculated previously using the finite element program *GTSTRUDL* with element *IPLQ*, which is a four-noded isoparametric linear quadrilateral element (Ioannides and Sengupta 2003). Results obtained confirmed the near perfect agreement between the two codes, thereby allowing the earlier research to be connected seamlessly to the work presented in this paper using *ABAQUS/STANDARD.*

Fracture Analysis of Beams Using Built-in Capabilities of *ABAQUS/STANDARD*

A number of built-in fracture mechanics capabilities are available in *ABAQUS*, including crack propagation analysis, tension softening models, contour integral evaluation (which includes the use of *Quarter-Point* elements), and material model *CONCRETE* (Hibbitt *et al*. 1994); the most promising of these, crack propagation analysis, is examined in this section. (A similar approach had been used by Gylltoft (1991) dealing with FCM implementation using *ABAQUS*.) Two simply supported beams are considered, as follows: Beam A (also used for linear elastic analyses), 406x152x38 mm (16x6x1.5 in.); and Beam B (for which experimental data are provided by Liu, 1994), 305x76x25 mm (12x3x1 in.). Because crack propagation analysis in *ABAQUS/ STANDARD* does not accommodate unnotched beams, only notched specimens are examined. Each of the two beams is tested with six different notch ratios, (a/h), ranging from 6.25% to 31.25% for Beam A, and between 6.67% to 66.67% for Beam B. Both beams are subjected to a concentrated load applied at their respective mid-spans. For Beam A, the modulus of elasticity, E, is 27.6 GPa (4000 ksi) with a Poisson's ratio, μ, of 0.15; and the tensile strength, f_t, is 3.2 MPa (0.463 ksi) (Ioannides and Sengupta 2003). The parameters for Beam B are identical to those for Beam A, except that the modulus of elasticity of the former is 37.3 MPa (5405 ksi), per Liu (1994).

Because the beams, the boundary conditions and the applied load are symmetric, only half of the structure needs to be considered. Thus, the half of each beam is subdivided into a variety of meshes to test the sensitivity of the solution to the mesh design. A baseline mesh is selected for each of the two half beams, as follows: Beam A: 64x48 elements, a/h = 16.67%; and Beam B: 30x15 elements, a/h = 33.33%. The length, a, along the symmetry line of both notches is 25 mm (1 in.).

The beam surfaces on either side of the symmetry line are specified as the planes along which the crack will propagate. They are first defined as a pair of contact surfaces and subsequently as a contact pair, consisting of the right side of the symmetry plane as the "slave surface" and the left as the "master surface." In the case examined here, the choice of master and slave surfaces is not significant and could be reversed without penalty.

The selection of the loading parameters was described in the previous section. That approach was found to work well for most of the cases considered. Another approach for the selection of the loading parameters may be to require that the linear elastic part of the response be completed in about 0.30 relative units of time, i.e., 30% of the total time, and that this portion entail about 10 time increments, each lasting 3E-2 relative units of time. The ITI may then be set at about 1/3rd of this value (1E-2), the MnTI at about 1/5th of the initial (2E-3), and the MxTI at about 5 times the initial (5E-2). This approach appears to lead to increments twice as large as those obtained by the previous approach, and would be very useful if the specified number of increments, e.g., 50, proved to be too small to allow the fracture process to proceed well beyond the peak loading point.

Neither of the two approaches outlined provides more than an initial guideline to the selection of the loading parameters. The sensitivity of the solution to values of input parameters selected in a broad range on either side of the values so determined was then examined. The responses tracked to study the effects of the loading parameters are the Peak Force (P_{max}) applied; the Load Line Deflection, LLD, calculated as the vertical displacement of the node of the load application at the center of the top of the beam; and half of the Crack Mouth Opening Displacement (CMOD), calculated as the horizontal displacement of the node at the center of the bottom of the beam. It became apparent that the loading parameters have a minor influence on the results, at least in the range of values investigated here for Beam A.

Runs were preformed to investigate the sensitivity of the solution to mesh fineness effects. All elements used were square, thereby eliminating any aspect ratio effects. Consequently, in all cases considered, the same loading parameters were used. It is observed in Table 1 that upon mesh refinement, all three of the responses tracked decrease, i.e., they converge to their respective finest mesh values from above. A fineness ratio of approximately 2-3% is recommended.

Table 1. Effect of mesh fineness

Beam A

Mesh	Peak Force (kips)	Percent Change	LLD (in.)	Percent Change	CMOD/2 (in.)	Percent Change
64 x 48	0.4720	0.00%	1.8554E-03	0.00%	3.1434E-04	0.00%
32 x 24	0.5373	13.83%	1.9505E-03	5.13%	3.6328E-04	15.57%
16 x 12	0.6909	46.38%	2.1670E-03	16.79%	4.0533E-04	28.95%
8 x 6	0.9259	96.17%	2.7734E-03	49.48%	4.7584E-04	51.38%

Beam B

Mesh	Peak Force (kips)	Percent Change	LLD (in.)	Percent Change	CMOD/2 (in.)	Percent Change
30 x 15	0.1260	0.00%	1.1754E-03	0.00%	2.5570E-04	0.00%
18 x 9	0.1550	23.02%	1.3673E-03	16.33%	2.7828E-04	8.83%
12 x 6	0.2007	59.29%	1.5154E-03	28.93%	2.6406E-04	3.27%
6 x 3	0.3007	138.65%	3.7537E-03	219.36%	1.8132E-04	29.09%

Note: 1 in. = 25.4 mm; 1 kip = 1000 lbs = 4448 N

The effects of element aspect ratio, α, are considered using two separate series of runs. Starting with the baseline cases for each of beams A and B, the first series considers the aspect ratio as the vertical dimension, Δy, of the element increases, whereas as the second tracks the responses as the horizontal dimension, Δx, is increased. In both cases, the other dimension is held constant. The loading parameters are also sensitive to changes in element aspect ratio; for convenience, however, one set of parameters that would satisfy the requirements for every run performed was selected and used for all analyses considered here. It is observed in Table 2 that the general trend is an increase in all three responses tracked as the aspect ratio in the y-direction increases while the aspect ratio in the x-direction remains constant, for both Beams A and B. A number of surprising results were also observed, however, particularly deviations form the general trend in the LLD, for both Beams A and B. In order to avoid such effects, it is required that fine meshes are used consisting of square elements. A similar investigation was performed in which the aspect ratio in the y-direction remained constant while the aspect ratio in the x-direction increased, producing the same general trends (see Table 3).

Table 2. Effect of aspect ratio in y-direction, α_y (Δx is constant)

Beam A

Mesh	α_y	Peak Force (kips)	Percent Change	LLD (in.)	Percent Change	CMOD/2 (in.)	Percent Change
64 x 48	1	0.4720	0.00%	1.8554E-03	0.00%	3.1434E-04	0.00%
64 x 24	2	0.4766	0.97%	1.6629E-03	10.38%	2.9667E-04	5.62%
64 x 12	4	0.6207	31.50%	1.9090E-03	2.89%	1.4473E-04	53.96%
64 x 6	8	0.9969	111.21%	3.2031E-03	72.64%	9.4465E-04	200.52%

Beam B

Mesh	α_y	Peak Force (kips)	Percent Change	LLD (in.)	Percent Change	CMOD/2 (in.)	Percent Change
30 x 15	1	0.1260	0.00%	1.1754E-03	0.00%	2.5570E-04	0.00%
30 x 9	1.67	0.1526	21.11%	1.9070E-03	62.24%	2.5790E-04	0.86%
30 x 6	2.5	0.1958	55.40%	1.5576E-03	32.52%	6.6888E-05	73.84%
30 x 3	5	0.3137	148.97%	2.9690E-03	152.59%	8.5476E-04	234.28%

Note: 1 in. = 25.4 mm; 1 kip = 1000 lbs = 4448 N

Table 3. Effect of aspect ratio in x-direction, α_x (Δy is constant)

Beam A

Mesh	α_x	Peak Force (kips)	Percent Change	LLD (in.)	Percent Change	CMOD/2 (in.)	Percent Change
64 x 48	1	0.4720	0.00%	1.8554E-03	0.00%	3.1434E-04	0.00%
32 x 48	2	1.3730	190.89%	6.7950E-03	266.23%	2.1413E-03	581.21%
16 x 48	4	0.6618	40.21%	2.6343E-03	41.98%	4.7782E-04	52.01%
8 x 48	8	0.7528	59.49%	3.7747E-03	103.44%	6.4841E-04	106.28%

Beam B

Mesh	α_x	Peak Force (kips)	Percent Change	LLD (in.)	Percent Change	CMOD/2 (in.)	Percent Change
30 x 15	1	0.1260	0.00%	1.1754E-03	0.00%	2.5570E-04	0.00%
15 x 15	2	0.1599	26.90%	1.5425E-03	31.23%	3.5023E-04	36.97%
10 x 15	3	0.1495	18.65%	1.5331E-03	30.43%	3.4779E-04	36.01%
6 x 15	5	0.1840	46.03%	2.1965E-03	86.87%	5.1830E-04	102.70%

Note: 1 in. = 25.4 mm; 1 kip = 1000 lbs = 4448 N

Next, the influence of notch size, quantified in terms of a/h, is considered, for the baseline values and ranges already noted for Beams A and B. The same loading and fracture process parameters are used for all these cases. Results in Table 4 indicate that the value of P_{max} decreases as the initial notch becomes deeper for both Beams A and B. On the other hand, the value of LLD decreases as a/h increases, indicating that the beams fail prematurely before they have a chance to deflect much.

Table 4. Effect of notch to beam thickness ratio, a/h

Beam A

a/h (%)	Peak Force (kips)	Percent Change	LLD (in.)	Percent Change	CMOD/2 (in.)	Percent Change
6.25	0.6426	36.14%	2.2850E-03	23.15%	2.1401E-04	31.92%
12.50	0.5206	10.30%	1.9635E-03	5.83%	3.4774E-04	10.63%
16.67	0.4720	0.00%	1.8554E-03	0.00%	3.1434E-04	0.00%
18.75	0.4479	5.11%	1.8171E-03	2.06%	3.9118E-04	24.44%
25.00	0.3724	21.10%	1.6624E-03	10.40%	4.2832E-04	36.26%
31.25	0.3136	33.56%	1.5504E-03	16.44%	4.6614E-04	48.29%

Beam B

a/h (%)	Peak Force (kips)	Percent Change	LLD (in.)	Percent Change	CMOD/2 (in.)	Percent Change
6.67	0.3303	162.14%	2.2118E-03	26.10%	7.8354E-04	206.43%
20.00	0.1927	52.94%	1.2839E-03	26.80%	5.4827E-04	114.42%
33.33	0.1260	0.00%	1.7540E-03	0.00%	2.5570E-04	0.00%
40.00	0.1036	17.78%	1.2052E-03	31.29%	7.0744E-04	176.67%
53.33	0.0687	45.45%	1.0142E-03	42.18%	3.3786E-04	32.13%
66.67	0.0400	68.28%	1.0350E-03	40.99%	3.8516E-04	50.63%

Note: 1 in. = 25.4 mm; 1 kip = 1000 lbs = 4448 N

These results are compared to those presented by Liu (1994) and by Sengupta (1998), the latter obtained using *CRACKIT* and rather coarse meshes, in order to limit the required number of executions of finite element program *GTSTRUDL*, which he had employed in deriving the flexibility matrices of the beams. For (half) Beam A, Sengupta's mesh consisted of 16x32 elements, i.e., the aspect ratio was 2.67; for Beam B, the mesh considered using *CRACKIT* was 12x15 elements, i.e., the aspect ratio was 2.5. In analyzing Beam A, Sengupta considered only an unnotched specimen; his stiffness matrix was modified during this study, enabling the investigators to examine Beam A assuming a variety of notch ratios ranging from 6.25% to 31.25%. Only one notch size is investigated using Beam B, namely 33.33%, which is the notch ratio also considered by Liu (1994) in his analysis of Beam B. The agreement between *ABAQUS* and *CRACKIT* was found to be better for Beam B than for Beam A. In the case of Beam B, near perfect agreement was observed for P_{max} and LLD. In contrast, a discrepancy of about 20% was observed in the results for CMOD. Upon further examination, this discrepancy is found to be due to the assumption implicit in *CRACKIT* that the notch remains undeformed until the crack begins to propagate. When the CMOD results from *CRACKIT* are increased by a constant amount corresponding to the horizontal displacement determined by ABAQUS at the time of first crack propagation, the *CRACKIT* results become practically identical to those form *ABAQUS*.

Beam A was analyzed with notch ratios ranging from 6.25% to 31.25%, α = 2.67, and mesh fineness in the vertical direction, $\Delta y/h$, of 3.1%. Comparisons of *ABAQUS* results with those from *CRACKIT* indicate that agreement is within about 20% for P_{max}, between 1 and 10% for LLD, and between 15 and 65% for CMOD. In an effort to unravel the sources of these discrepancies, some additional analyses are conducted. For the case of (a/h) = 6.25%, three runs using square elements of increasing fineness are performed, and these indicate that the corresponding results from the original run with a coarse mesh of 16x32 elements can be improved significantly. Assuming that the results from the finest square mesh ($\Delta y/h$ = 2%, α = 1) are a good indication of the exact solution, it is concluded that better estimates are obtained from *ABAQUS* than from *CRACKIT*, when both use the same coarse mesh, at least as far as P_{max} and LLD are concerned.

Results suggest that *CRACKIT* outperforms *ABAQUS* with regard to CMOD, but this is attributable to its implicit requirement that no CMOD develop before the first crack propagation. The same conclusion is reached when the coarse mesh results are compared to three runs involving aspect ratios, α, from 1 to 5.33. Additional confirmation is derived when similar mesh fineness comparisons for (a/h) values of 18.75% and 12.5% are conducted. These observations reinforce the credibility of the *ABAQUS* solution, but do not necessarily pin-point to the source of its discrepancies with *CRACKIT*, when the same coarse mesh is used. Possibilities include: (a) possible differences in the assumptions and formulations used in the two programs regarding the fracture process; and (b) possible shear locking experienced by the *CPS4* element. Results from *CPS4R* appear to be greatly influenced by the "hourglassing" phenomenon. Increasing the ABAQUS "hourglass stiffness" parameter to approximately the value of the Young's modulus of the beam material appears to relieve the problem considerably.

ABAQUS/STANDARD is used next to reproduce the experimental and theoretical data for Beam B presented by Liu (1994), who tested notched beams under quasi-static center-point loading, and compared his experimental results with those obtained from his own analytical procedure. In the experimental set-up used by Liu, the beam had a saw-cut notch along the centerline to promote cracking along the centerline; the notch-beam depth ratio was 33.33%. His specimens were made using natural sand, crushed limestone with 9.5-mm (3/8-in.) maximum size, Type I Portland cement, and water-cement ratio of 0.6; they were tested at 105 days. The other material properties used as inputs are E = 37.3 GPa (5,405,377 psi), G_f = 75.4 N/m (0.431 lb/in.), f_t = 3.2 MPa (463.27 psi) and μ = 0.15. As illustrated in Figure 1, very good agreement is obtained between the experimental and analytical results presented by Liu, and those predicted by *ABAQUS/STANDARD* employed in this study. Fifteen elements along the beam centerline are used in the present study, whereas Liu had used eighty elements. It is anticipated that using more elements along the beam centerline will yield an even more favorable comparison. Liu suggested that "a more sophisticated testing set-up" might also enhance the agreement between numerical and experimental data. For example, the wisdom of using a rather small maximum size of aggregate might be reconsidered. Nonetheless, it is gratifying that the procedure adopted is able to reproduce these data, despite this maximum aggregate limitation. The incorporation of the pre-existing notch along the beam centerline demonstrates the versatility of the numerical scheme used, and of the FCM itself.

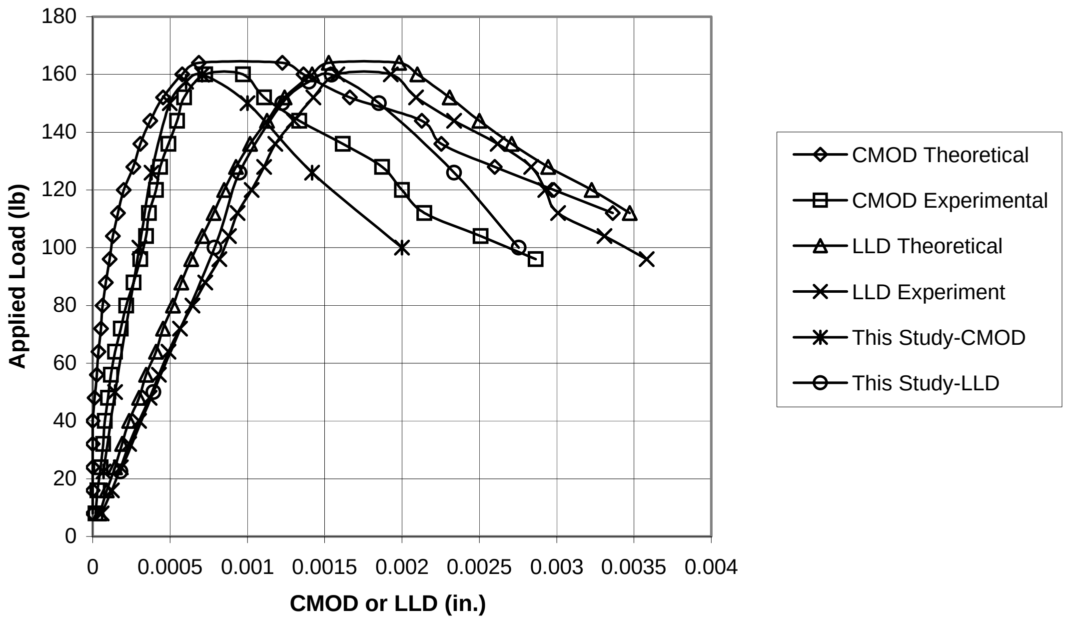

Figure 1. Comparison of experimental and theoretical results by Liu (1994) with those from this study (Note: 1 in. = 25.4 mm; 1 lb = 4.448 N)

Fracture Analysis of Beams Using *JOINTC* Elements in *ABAQUS/STANDARD*

The applicability of the built-in crack propagation analysis is restricted to 2D, symmetric, and notched cases. Consequently, this approach cannot be used to simulate crack propagation in 3D, arbitrarily loaded PCC pavement slabs, to be examined in subsequent stages of this on-going research. Therefore, an alternative formulation involving *JOINTC* elements is considered in this section, using a simply supported beam with the same dimensions and properties as Beam A from the previous section. The analytical methodology is derived for notched beam specimens. Unnotched specimens can be accommodated by assigning to them a small fictitious notch and compensating appropriately for this by increasing the tensile strength. Beam A is tested with six notch ratios, from 6.25% to 31.25% and is subjected to a concentrated load applied at its mid-span.

The experimental beam FCM bilinear curve employed by Liu (1994) is retained here. For this curve, critical CMOD, w_c = 0.085154 mm (0.0033525 in.); intersection point, (w_I, f_I) = (0.0189 mm, 0.1064988 MPa) or (0.000745 in., 0.1544233 ksi) ; for comparison purposes, a second, linear FCM curve with critical

CMOD, w_c = 0.047262 mm (0.0018607 in.) was also considered; both these curves correspond to fracture energy, G_f = 75.4 N/m (0.431 lb/in.).

Because the beam, the boundary conditions and the applied load are symmetric, only half of the structure needs to be considered, as previously explained. Thus, half of Beam A is subdivided into a series of uniform and non-uniform meshes, allowing direct comparison with results obtained by Sengupta (1998), and those from analyses discussed in the previous section. The element adopted in modeling the beam is the *CPS4*. In the previous section, which relied on the built-in capabilities of *ABAQUS/STANDARD*, the two surfaces included the notched portion of the beams, whereas now the notch surfaces are left untied. Except for this small difference, the approach followed here is identical to that adhered to earlier. The analysis does not involve large deformations or strains. Moreover, an infinitesimal rather than a small-sliding formulation is adopted, i.e., nonlinear geometric effects are also ignored.

Instead of specifying initially bonded conditions on the unnotched part of the slave surface through the use of a node set as in the previous section, pressure-clearance relationships for contact are extracted from the FCM curve and are adopted by modifying the default contact pressure-clearance relationship in an *ABAQUS* "mechanical contact" analysis. At each pair of nodes along the contact surfaces (which exclude the notch), *JOINTC* elements are then specified. *JOINTC* elements are used to model joint interactions and are made up of translational and rotational springs and parallel dashpots in a local, co-rotational coordinate system. By relying almost exclusively on the P-δ curve used in the definition of the nonlinear springs of the *JOINTC* element, the physical interpretation of the fracture process is facilitated considerably. In addition to using *JOINTC* elements, the application of *SPRING2* elements is briefly discussed in a subsequent paragraph.

The loading parameters in this section were chosen in accordance with the findings of the linear elastic section. Analyses were conducted to examine the influence of the maximum vertical displacement to be achieved, w_{max}, which indicate that improved precision is attained when w_{max} is reduced. For both values of the w_{max} considered in Table 5, however, results show that the LLD remains roughly the same despite changes in mesh fineness, suggesting that the resolution with which the fracture curve is tracked is too coarse. This means that the number of increments, estimated by the first of the aforementioned methods to be 30 (and which is actually 37 for the cases in Table 5), needs to be increased. An additional series of runs was then conducted aimed at doubling the number of increments. The MxTI, MnTI, and ITI are all halved for this purpose. The resolution with which LLD was tracked improved, but the execution time was almost doubled.

The baseline case considered for mesh fineness effects employs a 64x48 mesh for the half beam. All elements used are square, thereby eliminating any aspect ratio effects, which will be discussed separately in the following paragraph. The a/h ratio is set at 16.67%, and the bilinear FCM curve is employed. The time increments are: ITI = 0.006, MnTI = 0.0005, and MxTI = 0.03. These parameters result in 37 increments for the entire fracture process. Moreover, it is noted that in all cases, w_{max} is assumed to be 0.13 mm (0.005 in.), which is approximately twice as large as the LLD at peak force reported by Sengupta (1998) for these cases. Restricting the

Table 5. Influence of maximum vertical displacement to be achieved, w_{max}

Mesh	Element Size (in.)	w_{max} (in.)	Peak Force (kips)	LLD (in.)	CMOD/2 (in.)
64 x 48	1/8 x 1/8	0.03	0.6010	1.6425E-03	3.3987E-04
		0.005	0.6315	1.9238E-03	4.9172E-04
32 x 24	1/4 x 1/4	0.03	0.6578	1.6425E-03	3.6546E-04
		0.005	0.6783	1.7738E-03	4.3869E-04
16 x 12	1/2 x 1/2	0.03	0.7793	1.6425E-03	3.0879E-04
		0.005	0.7743	1.7738E-03	3.9237E-04
8 x 6	1 x 1	0.03	0.8301	1.6425E-03	2.6759E-04
		0.005	1.0700	2.2238E-03	5.0879E-04

Note: 1 in. = 25.4 mm; 1 kip = 1000 lbs = 4448 N

magnitude of this displacement allows a higher resolution for studying the fracture process at and in the immediate vicinity of the peak force. It is observed that upon mesh refinement, the peak force, P_{max}, decreases, while the other two responses tracked, LLD and CMOD, increase, i.e., the latter converge to their respective finest mesh values from below. The coarsest case produces results that are inconsistent with these general trends, possibly indicating that the solution degenerates when an inadequate number of *JOINTC* elements are provided. A fineness ratio of approximately 2-3% is recommended.

The effects of aspect ratio are considered using two separate series of runs. Starting with the same baseline case as adopted for the mesh fineness study above, the first series considers the aspect ratio as the vertical (beam thickness-wise) dimension of the element increases, whereas the second tracks the responses as the horizontal (beam length-wise) dimension is increased. In both cases, the other dimension is held constant. For the first series, the P-δ relationship for the *JOINTC* elements changes as the vertical node spacing, Δy, increases; in contrast, no such changes are necessary for the second series, since Δy remains unaltered for those runs. The time and load increments are not dependent on the mesh characteristics. Results presented in Table 6a illustrate the aspect ratio effects as the element vertical dimension increases. It is observed that the general trend is an increase in all three responses tracked as the aspect ratio increases, but this trend may be violated unpredictably when the number of *JOINTC* elements used decreases below some threshold value. This observation is confirmed by Table 6b, which shows results as the horizontal dimension of the element increases. All three responses tracked appear to be quite insensitive to the changes in the mesh because the vertical node spacing, Δy, and the corresponding number of *JOINTC* elements used remain unchanged. A minimum of 24 *JOINTC* elements is recommended.

As noted earlier, it is not possible to accommodate explicitly unnotched beam specimens using *JOINTC* elements. Consequently, a fictitious notch is introduced in unnotched specimens, and the change is compensated by adjusting the stiffness of adjoining *JOINTC* elements. The baseline case for the mesh fineness and aspect ratio investigations above considered an a/h value of 16.67% using 0.125 x 0.125 in. (3.2 x 3.2 mm) elements. In this paragraph, additional analyses are presented to investigate the effect of a/h on the responses obtained. The same time increments are used for all these cases. It was determined that the value of P_{max} decreases and the CMOD increases as the notch size increases, as might have been anticipated, since the notch is a plane of weakness, for notch ratios ranging from 0% to 31.25%. On the other hand, the value of LLD decreases as a/h increases, indicating that the beams fail prematurely before they have a chance to deflect much. The value of CMOD remains unchanged for several of the runs examined, suggesting that the fracture curve needs to be refined for higher resolution, possibly by setting the MxTI to a lower value.

Table 6a. Influence of aspect ratio in y-direction, α_y (Δx is constant)

Mesh	Element Size (in.)	α_y	Peak Force (kips)	LLD (in.)	CMOD/2 (in.)
64 x 48	1/8 x 1/8	1	0.6315	1.9238E-03	4.9172E-04
64 x 24	1/8 x 1/4	2	0.6822	2.0738E-03	6.4436E-04
64 x 12	1/8 x 1/2	4	0.7872	1.7738E-03	3.3708E-04
64 x 6	1/8 x 1	8	1.0470	2.3738E-03	1.1893E-03

Table 6b. Influence of aspect ratio in x-direction, α_x (Δy is constant)

Mesh	Element Size (in.)	Aspect Ratio, α_x	Peak Force (kips)	LLD (in.)	CMOD/2 (in.)
64 x 48	1/8 x 1/8	1	0.6315	1.9238E-03	4.9172E-04
32 x 48	1/4 x 1/8	2	0.6224	1.7738E-03	4.8408E-04
16 x 48	1/2 x 1/8	4	0.6204	1.7737E-03	5.3076E-04
8 x 48	1 x 1/8	8	0.6202	1.6237E-03	5.2516E-04
4 x 48	2 x 1/8	16	0.7026	1.6237E-03	2.4963E-04
2 x 48	4 x 1/8	32	0.6857	1.4737E-03	3.8340E-04

Note: 1 in. = 25.4 mm; 1 kip = 1000 lbs = 4448 N

Attempts were again made to reproduce results obtained using computer program *CRACKIT*, reported by Sengupta (1998). In analyzing Beam A, Sengupta considered only an unnotched specimen; the stiffness matrix used was modified during this study, enabling the investigators to examine Beam A assuming a variety of notch ratios ranging from 0% to 31.25%. The agreement between the built-in capabilities of *ABAQUS/ STANDARD* and the *JOINTC* model employed appears to be better for P_{max} and LLD than for CMOD. Percent agreement for these responses ranges from 102 to 110%, 98 to 115%, and 78 to 111%; respectively. Agreement between the *ABAQUS JOINTC* model and *CRACKIT* is somewhat less tight, ranging from 84 to 89%, 94 to 106% and 96 to 157%, respectively. It was noted in the previous section that such discrepancies are found to be due to the assumption implicit in *CRACKIT* that the notch remains undeformed until the crack begins to propagate. The conclusion reached earlier that better estimates are obtained from *ABAQUS* than from *CRACKIT* is reiterated here.

In the preceding cases, the bilinear FCM curve was employed. It is expected that using the bilinear curve simulates more closely results obtained in the laboratory.

It is interesting, however, to compare results obtained in this fashion to those generated using the simpler linear FCM curve. The condition of equivalency of the two hinges on retaining the same area under each of the curves, and setting this equal to G_f. Table 7 compares the tracked responses obtained using the two curves for two a/h ratios, small and large, and for two mesh designs, coarse and fine. It is observed that in general, the linear curve leads to higher responses than the bilinear curve. The P_{max} is about 10% higher, especially for the higher a/h and for the finer mesh. The LLD is about 25% higher, especially for the higher a/h and for the finer mesh. In contrast, CMOD is about 50% higher or 15% lower, indicating pronounced sensitivity to both a/h and mesh fineness, but not in a clearly discernible trend. A similar comparison using results from the built-in capabilities of *ABAQUS/ STANDARD* show that the P_{max} is again about 10% higher, the LLD is about 45% higher, and the CMOD is about to 90% higher or 2% lower. No clear explanation for these trends is available.

Table 7. Comparison of linear and bilinear FCM curves

Mesh	Element Size (in.)	a/h (%)	FCM Curve	Peak Force (kips)	LLD (in.)	CMOD/2 (in.)
8 x 6	1 x 1	16.67	Bilinear	1.0700	2.2238E-03	5.0879E-04
8 x 6	1 x 1	16.67	Linear	1.0890	2.2238E-03	5.1044E-04
8 x 6	1 x 1	33.33	Bilinear	0.7105	2.2238E-03	7.7711E-04
8 x 6	1 x 1	33.33	Linear	0.7722	2.3738E-03	6.2071E-04
64 x 48	1/8 x 1/8	16.67	Bilinear	0.6315	1.9238E-03	4.9172E-04
64 x 48	1/8 x 1/8	16.67	Linear	0.6867	2.3738E-03	7.2948E-04
64 x 48	1/8 x 1/8	33.33	Bilinear	0.4117	1.7738E-03	6.6379E-04
64 x 48	1/8 x 1/8	33.33	Linear	0.4488	2.0738E-03	8.1298E-04
64 x 48	1/8 x 1/8	16.67	Bilinear	0.6339	1.9368E-03	4.9971E-04
64 x 48	1/8 x 1/8	16.67	Linear	0.6889	2.3119E-03	6.8618E-04

Note: 1 in. = 25.4 mm; 1 kip = 1000 lbs = 4448 N

The primary tool for the model examined in this section is the *JOINTC* element, which is one of the spring-type elements available in *ABAQUS/STANDARD* that allow the user to define explicitly the desired fracture process. There are three main classes of such spring-type elements, namely *SPRING*, ITS (tube support elements), and *JOINTC* (flexible joint element). The stiffness (force per relative displacement) for all these is defined using the "*SPRING" option. *SPRING* elements include three distinct types: *SPRING1*, *SPRING2*, and *SPRINGA*, and all three can be linear or nonlinear. *SPRING1* is a spring between a node and the ground, acting in a fixed direction and is not useful at this time. *SPRING2* and *SPRINGA* connect two nodes, but whereas the first acts in a fixed direction, the line of action of the second can rotate, as might be necessary in large displacement analyses. Moreover, *SPRINGA* requires that the two nodes it connects be separated by a finite distance, whereas *SPRING2* can connect two nodes that occupy the same geometrical location. ITS elements are not relevant to this work. *JOINTC* elements consist of translational and rotational springs and connect two nodes that are essentially at the same geometric location, thereby dispensing with the need to define a spring length.

It is found that when *ABAQUS/STANDARD* is used, *SPRINGA* appears to be sensitive to the choice of spring length, for which no rational method of determination could be devised. Analyses were conducted to compare the behavior of *SPRING2* and *JOINTC* elements, and to justify the choice of the latter in this study. Table 8 compares the responses tracked using *SPRING2* and *JOINTC* elements with the bilinear curve for two a/h ratios, small and large, and for two mesh designs, coarse and fine. It is observed that the two element types give very similar results. In fact, for P_{max} and for LLD, results are identical; the CMOD results are within 5%. These data reinforce the credibility of the model using the *JOINTC* element. The latter was chosen because the plot of the deflected shape produced by *ABAQUS/POST* is more attractive. There is no other compelling reason to pick one over the other.

Table 8. Comparison between *JOINTC* and *SPRING2* elements

Mesh	Element Size (in.)	Element Type	a/h (%)	Peak Force (kips)	LLD (in.)	CMOD/2 (in.)
8 x 6	1 x 1	*JOINTC*	16.67	1.0700	2.2238E-03	5.0879E-04
8 x 6	1 x 1	*SPRING2*	16.67	1.0700	2.2238E-03	4.6835E-04
8 x 6	1 x 1	*JOINTC*	33.33	0.7105	2.2238E-03	7.7711E-04
8 x 6	1 x 1	*SPRING2*	33.33	0.7105	2.2238E-03	9.6497E-04
64 x 48	1/8 x 1/8	*JOINTC*	16.67	0.6315	1.9238E-03	4.9172E-04
64 x 48	1/8 x 1/8	*SPRING2*	16.67	0.6315	1.9238E-03	5.1544E-04
64 x 48	1/8 x 1/8	*JOINTC*	33.33	0.4117	1.7738E-03	6.6379E-04
64 x 48	1/8 x 1/8	*SPRING2*	33.33	0.4117	1.7738E-03	6.5433E-04

Note: 1 in. = 25.4 mm; 1 kip = 1000 lbs = 4448 N

Analyses were conducted to examine the influence of a progressively coarser mesh away from the notch region. As long as the aspect ratio in the x-direction, α_x, is below about 10, the three tracked responses remain unaffected. In contrast, the aspect ratio in the y-direction, α_y, can be as high as 100 or more, without significant deterioration in the results. Note that for the cases considered, the detrimental α_x-values occur near the crack tip.

Conclusion

This paper focuses on the application of the commercial software finite element package *ABAQUS/STANDARD* to tracking crack propagation in simply supported PCC beams. For any desired combination of beam and notch sizes, the crack propagation can be tracked by changing the input parameters for *ABAQUS* , thereby obviating the need for expensive laboratory tests. A well-designed factorial of such runs may then be performed in order to examine the specimen size effect over a wide range of input values.

Following a brief literature review, a study of the linear elastic behavior of simply supported beams is conducted. A comparison is made between the results obtained using *ABAQUS/STANDARD* with element *CPS4* and those calculated previously using the finite element program *GTSTRUDL* with element *IPLQ*. Results obtained confirm the near perfect agreement between the two codes, thereby allowing the earlier research to be connected seamlessly to the work presented in this paper using *ABAQUS/STANDARD*.

The most promising of the built-in fracture mechanics capabilities available in *ABAQUS*, namely crack propagation analysis, is examined next. Results are used to establish guidelines for the effective use of the code, and to verify the robustness of the formulation used. Satisfactory agreement is obtained with both analytical and laboratory results obtained in previous investigations. Finally, an alternative formulation is developed using the *JOINTC* element, anticipating the extension of the methodology followed in this paper to the case involving 3D PCC pavement slabs. Once again, user guidelines are established, leading to results that compare favorably with those reported from earlier studies, numerical and experimental.

This paper demonstrates that through a painstaking, step-by-step approach, a sophisticated analytical approach for concrete beams (and, therefore, presumably also for pavements) is feasible using a commercially available code. It is hoped that the use of fracture mechanics concepts in such a procedure will eventually lead to the definition of a more reliable and realistic mechanistic failure criterion, that will address the current weaknesses of transfer functions commonly employed in pavement design guides.

References

Bache, H. H. and I. Vinding (1990), "Fracture Mechanics in Design of Concrete Pavements," *Proceedings, Second International Workshop on the Design and Evaluation of Concrete Pavements, CROW/PIARC*, Sigüenza, Spain, 4-5 October, 139-164.

Gettu, R. and S. P. Shah (1994), "Fracture Mechanics." *High Performance Concrete: Properties and Applications*, Shah, S. P. and Ahmad, S. H. (Eds.), McGraw-Hill, Inc., New York, NY, 161-212.

Gylltoft, K. (1991). "Fracture Mechanics Analyses Using ABAQUS." *Proceedings of the International RILEM Workshop*, Elfgren, L. and Shah, S.P. (Editors). RILEM Proceedings No. 6, London, U.K., 152-159.

Hibbitt, Karlsson and Sorenson, Inc., (1994). "*ABAQUS/STANDARD* User's Manual." General Purpose Finite Element Analysis Program. Version 5.6. Pawtucket, RI.

Hillerborg, A., M. Modeer, and P. E. Petersson. (1976). "Analysis of Crack Formation and Crack Growth in Concrete by Means of Fracture Mechanics and Finite Elements." *Cement and Concrete Research*, 6(6), 773-792.

Ioannides, A. M. (1997a) "Fracture Mechanics in Pavement Engineering." *Transportation Research Record 1568, TRB, National Research Council*, Washington, DC, 10-16.

Ioannides, A. M. (1997b). "Pavement Fatigue Concepts: A Historical Review." *Proceedings of the Sixth International Purdue Conference on Concrete Pavement Design and Materials for High Performance*, Vol. 3, Indianapolis, Indiana, 147-159.

Ioannides, A. M., S. Peng, and S. Sengupta. (2003). "Crack Propagation in Portland Cement Concrete: Combining Dimensional Analysis and Finite Elements." *Proceedings of the International Conference on Highway Pavement Data, Analysis and Mechanistic Design Applications*, Vol. 1, Columbus, Ohio, 271-279.

Ioannides, A. M. and S. Sengupta. (2003). "Crack Propagation in Portland Cement Concrete Beams: Implications for Pavement Design." *Transportation Research Record 1853, TRB, National Research Council*, Washington, D. C., 110-117.

Liu, P. (1994). "Time-Dependent Fracture of Concrete." Ph.D. dissertation. Ohio State University, Columbus, Ohio.

Sengupta, S. (1998). "Finite Element Simulation of Crack Growth in PCC Beams: Implications for Concrete Pavement Design." M.S. thesis. University of Cincinnati, Cincinnati, Ohio.

List of Symbols

α = element aspect ratio
α_x = element aspect ratio in the x-direction (horizontal or beam length-wise)
α_y = element aspect ratio in the y-direction (vertical or beam thickness-wise)
a = notch depth
CMO = Crack Mouth Opening
CMOD = Crack Mouth Opening Displacement
δ = deflection
Δx = element dimension in x-direction
Δy = element dimension in y-direction
E = modulus of elasticity
FCM = Fictitious Crack Model
f_I = intersection point coordinate for strength on FCM bilinear curve

f_t = tensile strength
G_f = fracture energy
h = beam thickness
ITI = Initial Time Increment
LLD = Load Line Displacement
μ = Poisson's ratio
MnTI = Minimum Time Increment
MxTI = Maximum Time Increment
P = applied load
PCC = Portland Cement Concrete
P_{max} = peak force
TPS = Time Period of Step
w_c = critical Crack Mouth Opening
w_I = intersection point coordinate for Crack Mouth Opening on FCM bilinear curve
w_{max} = maximum vertical displacement to be achieved ■